MÖSSBAUER SPECTROSCOPY OF ^{125}Te - SOME NEW RESULTS AND APPLICATIONS

P. Boolchand,* B. B. Triplett and S. S. Hanna

Department of Physics
Stanford University
Stanford, California 94305†

and

J. P. deNeufville

Energy Conversion Devices, Inc.
Troy, Michigan 48084

Narrow and reproducible linewidths for the 35.5-keV Mössbauer resonance in ^{125}Te have been observed with a 2.7-year ^{125}Sb source diffused in Cu. Measurements made on cubic ZnTe as a function of absorber thickness reveal that the linewidth of these sources is $\Gamma_{source} = 5.20 \pm 0.08$ mm/sec. This result is in good agreement with the minimum observable linewidth $2\Gamma_{nat}$ as calculated from the measured half-life of the 3/2 level, $t_{1/2} = 1.475 \pm 0.010$ nsec. From this Mössbauer measurement the Debye temperature of cubic ZnTe is found to be 175 ± 9 °K. The Mössbauer effect in ^{125}Te provides a useful technique for characterizing amorphous chalcogenide semiconductors. Investigations on sputtered thin films of amorphous Ge_xTe_{1-x} were performed as a function of composition, temperature, and heat treatment. The variation of the quadrupole splitting as a function of composition exhibits discontinuities in slope at $x = 0.33$ and

---

* Permanent address: University of Cincinnati, Cincinnati, Ohio 45221

† Supported in part by the National Science Foundation.

0.50. These results are indicative of chemical ordering in the amorphous Ge_xTe_{1-x} system at these compositions. A structural model of amorphous Ge_xTe_{1-x} alloys based on two inequivalent Te sites is developed for the Te rich phase and is found to fit the data well. Annealing of the films is shown to lead to a greater degree of structural order on a microscopic scale. Crystallizing the films is shown to lead to phase separation of the system into crystalline GeTe and Te metal.

INTRODUCTION

Investigations of the 35.5-keV gamma resonance in ^{125}Te have primarily been based on the use of ^{125}I ($t_{1/2}$ = 60 days) in Cu and ^{125m}Te ($t_{1/2}$ = 58 days) in ZnTe as sources of monoenergetic gamma rays. Both these sources are known to exhibit broad linewidths, and in particular the linewidths of ^{125}I sources are not reproducible. We now report that recent experiments [1,2] with ^{125}Sb (2.7 years) sources diffused in Cu demonstrate that these sources are characterized by a narrow and reproducible linewidth. Measurements [2] made on cubic ZnTe as a function of absorber thickness reveal that the linewidth of these sources agrees well with $2\Gamma_n$, the minimum observable linewidth based on the half life of the 3/2 level measured directly from its rate of decay [3]. These experiments have also shown that the Mössbauer f factor of ^{125}Sb sources is substantially larger than for ^{125}I sources. The combination of these favorable properties, viz., narrow linewidth, long parent half-life, and large f factor, makes an ^{125}Sb source particularly attractive for future Mössbauer effect work with ^{125}Te. The isomer shift of Te metal relative to this source is found to be +0.50 ± 0.04 mm/sec. We propose this source be used as a standard for ^{125}Te isomer shift measurements.

The significance of a narrow single-line source cannot be overemphasized for measurements of electric and magnetic hyperfine interactions. The ^{125}Te resonance has a natural linewidth $2\Gamma_n$ of 5.20 ± 0.04 mm/sec and the presence of hyperfine interactions lead invariably to partially resolved spectra. Reliable analysis of such spectra is possible only by giving due consideration to the linewidths of the unre-

solved components [4]. In this sense the present results offer the promise of higher precision in the study of the ^{125}Te gamma resonance.

A particularly important application of ^{125}Te spectroscopy is its use as a microscopic probe in the characterization of chalcogenide-amorphous semiconductors. The applied interest in these non-crystalline materials derives from the Ovonic Threshold Switching that these substances display. The nature of the bonding and structure in the amorphous Ge_xTe_{1-x} system has for this reason led to numerous investigations [5] involving a variety of techniques such as X-ray [6], neutron RDF [7], and XPS [8]. In this paper we present results on this system obtained with ^{125}Te Mössbauer spectroscopy. Amorphous thin films of Ge_xTe_{1-x} were used as absorbers, and experiments were performed as a function of composition and temperature of the films. Spectra of virgin and annealed films were also obtained to investigate the role of thermally induced changes in the structure of amorphous alloys. The amorphous films were crystallized by heating in vacuum above the crystallization temperature T_x. Crystallization of these films was found to produce crystalline GeTe and Te from the amorphous Ge_xTe_{1-x} system. The experimental procedure and results of the present investigations are summarized in the next section, where we also develop a structural model of amorphous Ge_xTe_{1-x} alloys in order to interpret the data. Substantial changes in the Mössbauer effect spectra of virgin and annealed amorphous Ge_xTe_{1-x} films suggest the existence of defect structures in the virgin films. It is believed that the process of annealing leads to formation of a greater degree of structural ordering.

The structure of amorphous Ge_xTe_{1-x} alloys has been the subject of numerous other physical measurements. Also, in the next section an attempt is made to discuss the existing semiclassical description of these alloys with the model developed from the Mössbauer measurements.

Predictions for the amorphous phase of Te, corresponding to composition $x = 0$ in Ge_xTe_{1-x}, are of particular interest. For amorphous Te, one infers a substantially larger quadrupole splitting and a smaller isomer shift than the value known for the crystalline form.

PROCEDURE, RESULTS, AND INTERPRETATION

Mössbauer effect spectra were accumulated by use of a constant acceleration drive with provisions for a simultaneous velocity calibration. The ^{125}Te spectra were recorded with an $^{125}Sb(\underline{Cu})$ source by detecting the K_α escape peak (5.8 keV) in a Xe filled proportional counter.

Linewidth Measurements on a $^{125}Sb(\underline{Cu})$ Source

Mössbauer spectra from an $^{125}Sb(\underline{Cu})$ source with ZnTe absorbers of different thicknesses were recorded. By linear extrapolation to zero absorber thickness one can eliminate contributions to the observed linewidth from absorber thickness. The cryostat used in these measurements provided both source and absorber cooling down to liquid nitrogen or helium temperatures by means of exchange gas system. Samples of ZnTe obtained from three suppliers were investigated separately. Sample A consisted of chips of cubic single crystals from Gould Industries, Cleveland, Ohio; sample B consisted of polycrystalline ZnTe, stated purity 99.999%, bought from Research Inorganic Chemical Corporation, Sun Valley, California; and sample C consisted or enriched $Zn^{125}Te$ hot pressed in a lucite matrix and was made available by New England Nuclear, Boston, Massachusetts.

The narrowest linewidths were observed for ZnTe absorbers made from sample A. These experiments were performed at 78°K and 4.2°K on the same set of absorbers. A summary of the linewidth data obtained as a function of absorber thickness appears in Fig. 1. The data were fit to a straight line and gave the following results.

$T = 4.2°K$	$\Gamma_{source} = 5.30 \pm 0.05$ mm/sec	$f_{ZnTe} = 0.57 \pm 0.01$
$T = 78°K$	$\Gamma_{source} = 5.10 \pm 0.08$ mm/sec	$f_{ZnTe} = 0.32 \pm 0.02$

The values of Γ_{source} are in good agreement with $2\Gamma_n = \hbar/\tau = 5.20 \pm 0.04$ mm/sec obtained from the measured [3] half life $t_{1/2} = 1.475 \pm 0.010$ nsec of the $3/2^+$ state. In a Debye model the measured f values of cubic ZnTe translate to a mean $\theta_D = 175 \pm 9°K$. Recently Blattner et al. [9] have reported an effective Debye temperature of $\theta_M = 180 \pm 6°K$ for cubic ZnTe from X-ray measurements.

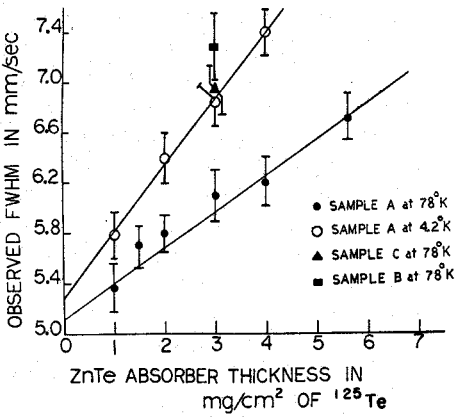

Fig. 1. Observed linewidth of a ^{125}Sb(Cu) source as a function of ZnTe absorber thickness in mg/cm^2 of ^{125}Te.

Sizable line broadening was observed in polycrystalline ZnTe samples B and C. For an absorber of ^{125}Te 3 mg/cm^2 thick, the linewidths for samples B and C were found to be 20% broader than those for sample A (Fig. 1). An X-ray examination of samples A and B showed additional peaks in sample B which can be identified as the hexagonal phase of ZnTe. The line broadening in sample B may thus be attributed to the existence of an unresolved quadrupole splitting in a non-cubic phase. Since the color of the cubic sample A was dull orange in contrast to the brown color or the other two samples, it is likely that the above explanation also applies to sample C.

The narrower emission linewidths of ^{125}Sb(Cu) sources compared with those of ^{125}I(Cu) and Zn^{125m}Te sources also deserve a few comments. It is known that Sb dissolves in Cu, although the same cannot be said for I in Cu. It is likely that CuI is formed during the electroplating and diffusion processing of I in Cu sources. It is known that CuI exists both in a cubic and non-cubic phase [10]. These observations suggest a possible explanation

for the lack of reproducibility of the linewidths that have been observed with $^{125}I(\underline{Cu})$ sources. For $Zn^{125m}Te$ sources on the other hand, failure to achieve natural linewidths, in the absence of resonant self-absorption in the source matrix, is due to the difficulty of achieving a purely cubic phase in polycrystalline ZnTe samples. These considerations on line broadening are also relevant to the Mössbauer spectroscopies of $^{127,129}I$ where matrices of ZnTe and Cu have been used to achieve single line sources or absorbers, or both.

Mössbauer Effect Measurements on the Ge_xTe_{1-x} System

Thin amorphous films of Ge_xTe_{1-x} were used as absorbers in conjunction with $^{125}Sb(\underline{Cu})$ sources. The measurements were performed under a variety of conditions which may be characterized by the following variables:

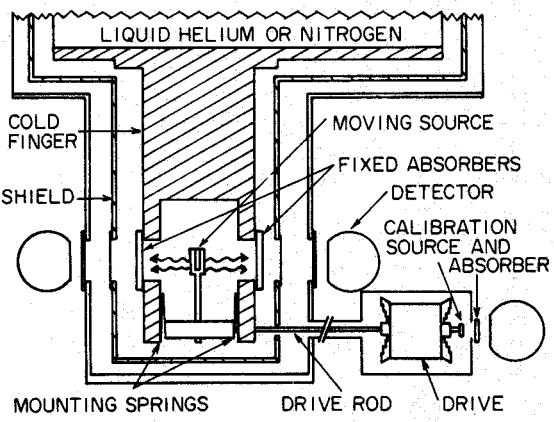

Fig. 2. Schematic drawing of the cold-finger cryostat and detector arrangement.

(i) Temperature

(ii) Composition

(iii) Heat treatment: annealing effects on amorphous films, and amorphous to crystalline phase transformations.

A novel feature of the method used in these measurements provided for calibrating the drive while simultaneously recording spectra of two absorbers maintained at cryogenic temperatures. Figure 2 illustrates the schematic arrangement of the experiment. The two absorbers and source were cooled by conduction by means of a Cu cold finger. The source was driven horizontally with a loudspeaker drive assembly which was calibrated at the far end by recording spectra from a $^{57}Co(\underline{Pt})$ source and 1 mil Fe metal absorber. Figure 3 reproduces spectra of K_2TeO_3 and Te metal obtained in a single run with the simultaneous Fe calibration. The present method is particularly attractive for comparing isomer shifts of different Te absorbers. Parameters derived from these data are summarized in Table I.

Table I. Parameters Derived from the Data in Figure 3

Absorber	Thickness mg/cm^2	Γ_{exp} mm/sec	Δ mm/sec	$\delta^\dagger$ mm/sec
ZnTe	2.80	6.50 ± 0.14	-	-0.15 ± 0.04
K_2TeO_3	4.00	6.52 ± 0.10	6.80 ± 0.05	+0.28 ± 0.05
Te	4.00	6.38 ± 0.11	7.78 ± 0.06	+0.52 ± 0.05

†The isomer shift δ is measured relative to the source, ^{125}Sb in Cu.

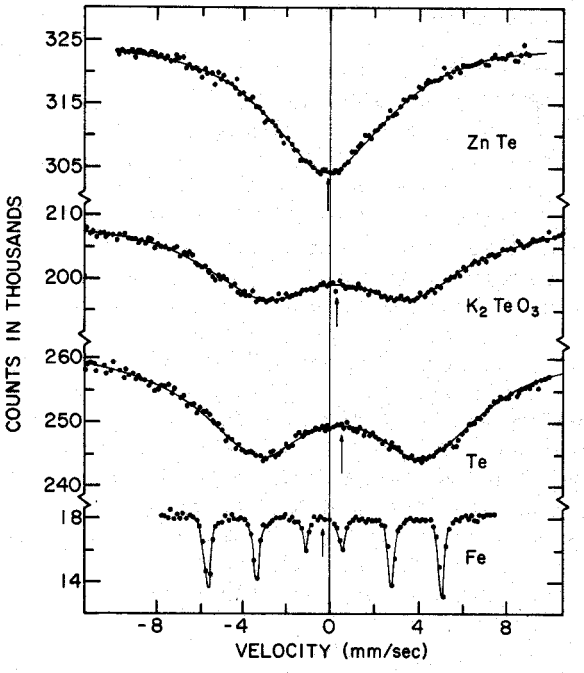

Fig. 3. Mössbauer spectra accumulated with a $^{125}Sb(\underline{Cu})$ source and the absorbers ZnTe, K_2TeO_3, and Te. Also shown at bottom is a spectrum taken with a $^{57}Co(\underline{Pt})$ source and a 1 mil Fe metal absorber.

Ge_xTe_{1-x} Absorbers

The amorphous films used in the present investigations were prepared at Energy Conversion Devices, Troy, Michigan by rf sputtering the material onto 15 μ thick Al foil substrates. Typical film thicknesses ranged from 5 to 50 μ. For the Ge rich composition, absorbers were prepared by stacking together a few films to achieve sufficient ^{125}Te thickness.

Temperature Measurements

The bulk of the Mössbauer effect measurements were performed at liquid helium temperature. In the preliminary phase of these experiments, however, some measurements were performed at 78°K to investigate whether the choice of substrate might produce significant changes in the spectra of amorphous Ge_xTe_{1-x} films. Figure 4 reproduces spectra of films sputtered on glass and Al substrates. In each case the spectra of the amorphous films were characterized by a weakly split quadrupole doublet which showed no significant substrate dependence either in splitting or linewidth.

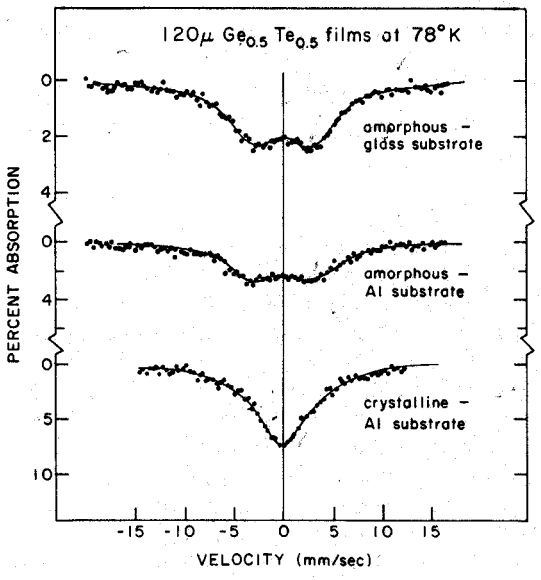

Fig. 4. Mössbauer spectra of 120 μ $Ge_{0.5}Te_{0.5}$ taken at 78°K. The upper two spectra were taken with amorphous films on glass and aluminum substrates, respectively. The lower spectrum was taken after crystallizing (see text) the film on the Al substrate.

Table II. Summary of ^{125}Te Mössbauer Effect Results on 120 μ Thick $Ge_{0.5}Te_{0.5}$ Absorbers at 78°K

Absorber	Substrate	Γ_{exp} (mm/sec)	% Effect	Area[a)]
Amorphous	glass	5.73 ± 0.20	1.95 ± 0.05	22.3 ± 1.0
Amorphous	Al	5.63 ± 0.20	2.28 ± 0.04	25.6 ± 1.0
Crystalline	Al	6.28 ± 0.17	7.13 ± 0.11	44.8 ± 1.5

a) Area under the resonance in arbitrary units. Note that for the Al substrate: $\frac{f_{crystalline\ Ge_{0.5}Te_{0.5}}}{f_{amorphous\ Ge_{0.5}Te_{0.5}}} = 1.75 \pm 0.13$.

An amorphous GeTe film on an Al substrate was crystallized by heating in vacuum to 250°C for about 6 hrs. A spectrum of the crystallized film (Fig. 4) showed a single line with a 7.1% dip (Table II). The area under the resonance for crystalline GeTe is a factor of 1.75 larger than that for amorphous GeTe. These measurements were performed in identical geometries with absorbers of the same thickness. For identical experimental conditions it is clear that the ratio of areas in the resonance reflects directly the ratio of f in the two absorbers. One thus concludes that f in amorphous GeTe is substantially lower than that in crystalline GeTe at 78°K. Measurements performed at liquid helium temperature show, however, that the f factors in amorphous and crystalline GeTe are approximately equal. We believe the strong temperature dependence of f in amorphous GeTe may be a manifestation of the resonant atom rattling in its site. This subject merits further study.

In this connection, recent measurements of the heat capacities of amorphous and crystalline Ge have shown them to be closely proportional at all temperatures below 30°K.

This result has led to the rather surprising suggestion [11] that the phonon density of states spectrum in amorphous Ge closely resembles the spectrum for the crystalline phase (but with all frequencies in the amorphous phase reduced by 16% in order to account for the ratio of the heat capacities). The strong temperature dependence of the ratio of the f values of amorphous and crystalline GeTe allows an immediate statement that for GeTe there cannot be such a similarity in the density of states spectra. Mössbauer f values probe a lower frequency region of the phonon spectrum than do heat capacity measurements [12]. For this reason, f values and heat capacities, together with Raman scattering and electronic tunneling, provide powerful, complementary probes of the structure of the vibrational spectra of amorphous materials.

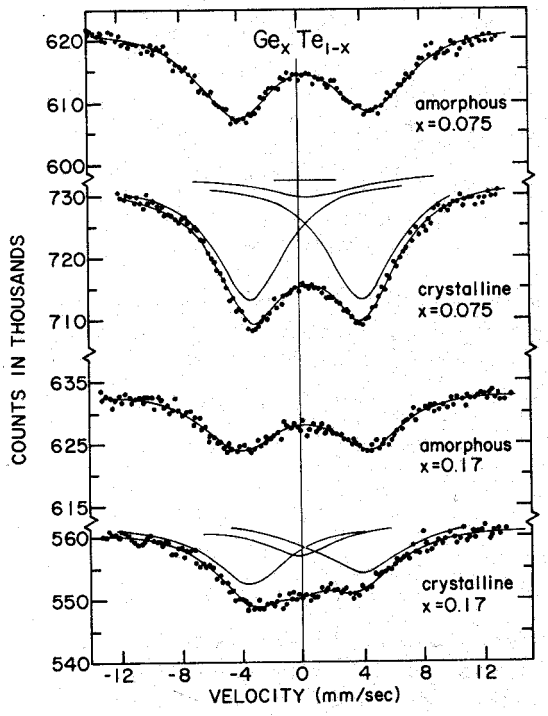

Fig. 5. Comparison of Mössbauer spectra taken on the amorphous and crystalline phases obtained from Ge_xTe_{1-x} for x = 0.075 (upper pair of spectra) and x = 0.17 (lower pair of spectra).

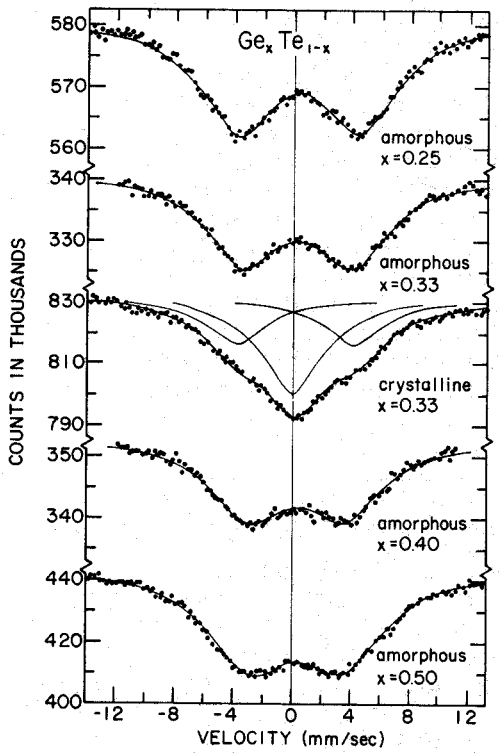

Fig. 6. Mössbauer spectra for amorphous Ge_xTe_{1-x} with x = 0.25, 0.33, 0.40 and 0.50. Shown for comparison in the middle of the figure is a spectrum for crystalline Ge_xTe_{1-x} with x = 0.33.

Our measurements exhibit the dramatic change in Te coordination in the amorphous to crystalline phase transformation of GeTe. The linewidth of the crystalline GeTe spectrum has now been investigated [13], and it cannot entirely be attributed to the effect of absorber thickness. One estimates that 6% of the linewidth in crystalline GeTe results from the presence of a non-vanishing electric field

gradient. This result is corroborated by X-ray examination of our sample which showed a slight (1.5%) rhombic distortion of the cubic unit cell.

The appearance of a quadrupole splitting (QS) in amorphous GeTe shows that the local coordination at Te in this host is less symmetric than in crystalline GeTe. In the amorphous GeTe spectrum, the linewidths of the components are quite broad and we attribute this to a distribution of QS's. This distribution may be due to inhomogeneous

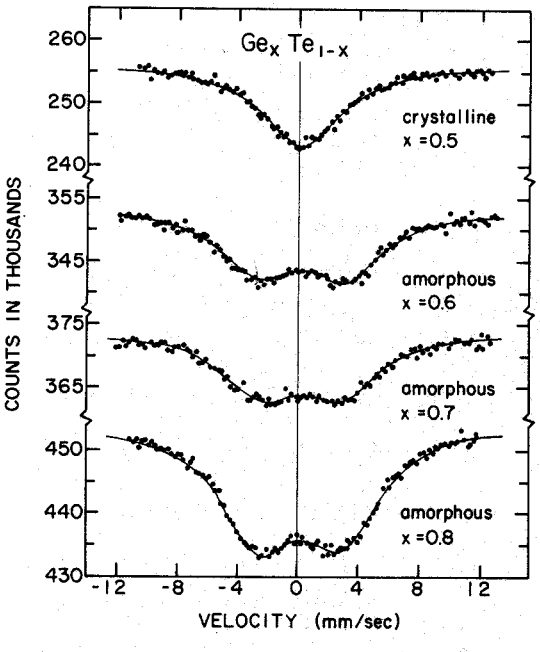

Fig. 7. Mössbauer spectra for amorphous Ge_xTe_{1-x} with x = 0.6, 0.7, and 0.8 compared with crystalline GeTe (upper spectrum).

distortions of the local coordination around the Te sites. These observations can be reconciled in terms of a three fold coordinated model for amorphous GeTe and will be discussed later on.

Composition

Spectra of freshly sputtered Ge_xTe_{1-x} films (virgin) are presented in Figs. 5, 6, and 7 sequentially with increasing Ge fraction. In all cases the spectra consisted of partially resolved doublets and were fit to a superposition

Table III. Parameters Derived from the Data in Figs. 5, 6, and 7 for Amorphous Films

Ge_xTe_{1-x} Absorber	Thickness mg/cm^2	Γ_{exp} mm/sec	Δ mm/sec	$\delta^\dagger$ mm/sec
x = 0.075	1.45	6.14 ± 0.11	9.34 ± 0.07	+0.38 ± 0.07
x = 0.17	0.53	6.58 ± 0.20	8.84 ± 0.11	+0.42 ± 0.12
x = 0.25	3.40	6.34 ± 0.10	8.42 ± 0.06	+0.30 ± 0.06
x = 0.33	3.17	6.46 ± 0.08	7.80 ± 0.04	+0.27 ± 0.05
x = 0.40	1.94	6.49 ± 0.11	6.85 ± 0.08	+0.26 ± 0.08
x = 0.50	1.07	6.60 ± 0.06	6.17 ± 0.04	+0.22 ± 0.03
x = 0.60	1.31	6.22 ± 0.12	6.17 ± 0.08	+0.16 ± 0.08
x = 0.70	1.43	6.17 ± 0.16	5.57 ± 0.08	+0.17 ± 0.08
x = 0.80	2.8	6.23 ± 0.10	5.68 ± 0.08	+0.22 ± 0.06

† The isomer shift δ is measured relative to the source, ^{125}Sb in Cu.

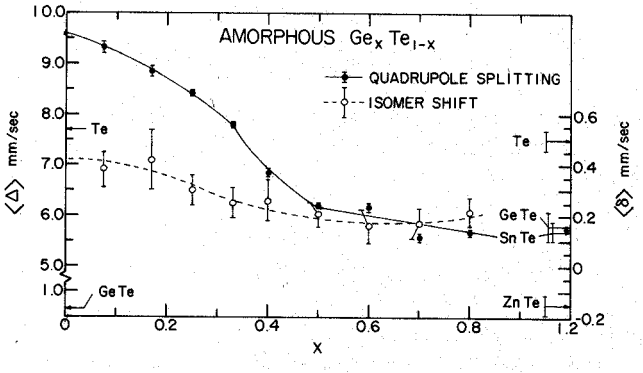

Fig. 8. Mean quadrupole splitting $\langle\Delta\rangle$ and isomer shift $\langle\delta\rangle$ for virgin amorphous Ge_xTe_{1-x} as a function of x.

of two Lorentzian line shapes to extract a mean quadrupole splitting $\langle\Delta\rangle$, isomer shift $\langle\delta\rangle$, and observed linewidth $\langle\Gamma_{exp}\rangle$ (Table III). The trends of $\langle\Delta\rangle$ and $\langle\delta\rangle$ as a function of composition are shown in Fig. 8.

The most striking features of these trends are the rapid and monotonic increase in $\langle\Delta\rangle$ for the composition range $x < 0.33$ and the existence of discontinuities in the slope of $\langle\Delta\rangle$ at the compositions $x = 0.33$ and 0.50. In the composition range $x > 0.50$, the $\langle\Delta\rangle$ values exhibit only a minor additional decrease in magnitude. In this region the rather large scatter in the values is primarily due to the fact that the doublet is only partially resolved. The composition $x = 0.17$ was studied with both a thick and a very thin absorber, with the hope that the thin absorber might lead to a reduction in the somewhat broadened linewidth. However, no significant improvement was found.

The Covalent Bond Length of Amorphous Te

The most Te rich amorphous composition investigated corresponded to $x = 0.075$. Smooth extrapolations of the $\langle\Delta\rangle$ and $\langle\delta\rangle$ values to $x = 0$ give

$$\Delta = 9.60 \pm 0.05 \text{ mm/sec}$$

$$\delta = +0.41 \pm 0.06 \text{ mm/sec}$$

These parameters are ascribed to amorphous Te. One notes that they are substantially different from those known [14] for crystalline Te:

$$\Delta = 7.74 \pm 0.04 \text{ mm/sec}$$

$$\delta = +0.50 \pm 0.03 \text{ mm/sec}$$

Since it is generally assumed that amorphous Te is predominantely two fold coordinated [15] as it is in the trigonal phase, it is necessary to explain this large difference in the extrapolated QS before attempting to advance a model describing the behavior of Ge_xTe_{1-x} as a function of x. We suggest that this phenomenon is related to the shorter covalent bond distance in amorphous Te.

It has been observed [16] that a linear relationship exists between the observed QS for Te(X) and R^{-3}, where R represents the length of the Te-X covalent bond and X represents orthorhombic S, trigonal Se, or trigonal Te. Figure 9 is reproduced from Ref. 16 and the straight line passing through the data represents the best fit to the QS as a function of R^{-3}.

In order to put amorphous points on Fig. 9, we need both Mössbauer QS measurements and direct measurements of the covalent bond distance in amorphous chalcogenides. Although no such Mössbauer measurements are yet available, indirect comparisons can be made with the amorphous compositions $Ge_{0.11}Te_{0.89}$ studied [17] by the X-ray radial distribution (RDF) technique and $Ge_{0.17}Te_{0.83}$ studied [7] with both X-ray and neutron RDF. Since these compositions are Te rich, and since the first-neighbor X-ray RDF peak is known [17] to be rather insensitive to composition, these comparisons should allow a good first approximation to amorphous Te. Accordingly, we have added to Fig. 9 our QS values for these compositions, with the first-neighbor RDF peak used to represent the covalent bond length. Two points are shown for the composition $Ge_{0.17}Te_{0.83}$ since the neutron and X-ray RDF give [7] peaks at 2.65 and 2.75 Å, respectively. This apparent discrepancy occurs because of the relative insensitivity to Ge in the X-ray technique leading to a heavier weighting of Te-Te

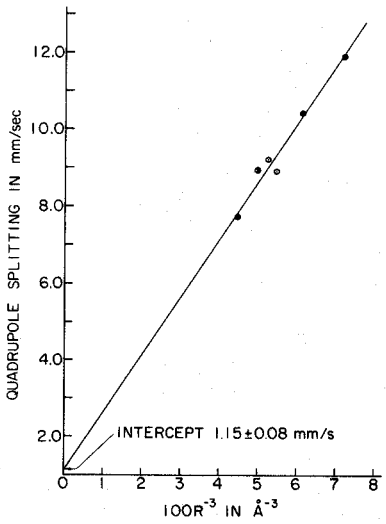

Fig. 9. Quadrupole splitting vs. R^{-3} where R represents the covalent bond length Te-X. Solid circles are for Te dissolved in crystalline hosts (Ref. 16). The amorphous points are for $Ge_{0.17}Te_{0.83}$ and $Ge_{0.11}Te_{0.89}$ and use for R the effective first neighbor distance from neutron RDF (circled cross) and X-ray RDF (circled dots). The errors in the QS measurements are less than the size of the circles.

bonds relative to the shorter Ge-Te bonds which are unresolved in both RDF spectra. The result appropriate to our observed Mössbauer QS values would be expected to be inbetween the two RDF values. In any case, we expect that the uncertainty in placing amorphous points on Fig. 9 will diminish when X-ray, neutron, and electron RDF data become available for amorphous Ge_xTe_{1-x} as a function of x.

We consider the data and the argument in Fig. 9 sufficiently convincing [18] to propose that our Mössbauer measurements indicate an effective covalent bond length of 2.62 Å for pure amorphous Te. However, it is not clear to us how this bond length, extrapolated from stabilized Ge_xTe_{1-x} films, may relate to the observed properties of the"amorphous" Te films prepared in the laboratory. For instance, a recent note [19] on the electron RDF of Te evaporated onto a substrate at liquid helium temperature shows a first near-neighbor position of 2.79 Å and suggests a two-fold coordinated chain length of about seven atoms.

The 2.79 Å bond distance, although less than the 2.8335 Å characteristic of trigonal Te, is clearly inconsistent with the current interpretation. This situation brings up the crucial question, originally raised in Ref. 15, of whether these "amorphous" Te films consist of randomly separated chains, form as fine microcrystalline trigonal crystals, or even exist in intermediate states having both microcrystalline and amorphous character. Considering the experimental uncertainty [20] surrounding the situation, we leave the question open.

Structural Ordering in the Amorphous Ge_xTe_{1-x} System

We propose that the discontinuities in the slope of the $\langle\Delta\rangle$ versus x curve (Fig. 8) at the compositions $x = 0.33$ and 0.50 result from the occurance of chemical ordering in the amorphous Ge_xTe_{1-x} system. At each of these compositions Te finds itself in an almost well defined local environment. Furthermore, we will show that the QS at the composition $x = 0.33$ becomes more or less definite on annealing the virgin amorphous films.

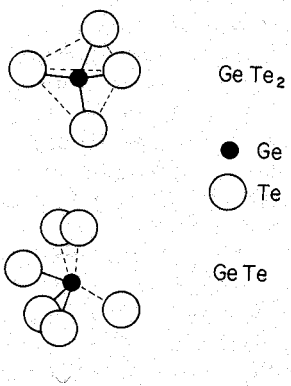

Fig. 10. Tetrahedral structure proposed in Ref. 21 for amorphous $GeTe_2$ (above) and the black phosphorus structure proposed in Ref. 22 for amorphous GeTe (below).

The smooth change in $\langle\Delta\rangle$ in the two composition ranges 0 to 0.33 and 0.33 to 0.50 originates, in our view, from a redistribution in the population of the inequivalent Te sites. It is also clear that one must invoke the presence of at least two inequivalent Te sites. In view of the simplicity of a structural model based on two inequivalent Te sites, it seems worthwhile to investigate its consequences.

At the composition $x = 0.33$ it is believed that $GeTe_2$ [21] exists in a structure similar to SiO_2. In this structure, the valence of each atom is locally satisfied in that each Ge is four-fold coordinated to Te, while each Te is two-fold coordinated to Ge. Figure 10 illustrates the $GeTe_2$ tetrahedron. At $x = 0.5$, it is believed that amorphous GeTe [22] exists in the black phosphorus structure. In this structure Te is coordinated to three first Ge neighbors and three second Ge neighbors (Fig. 10).

Two-Site Model of Amorphous Ge_xTe_{1-x} $(0 < x < 0.5)$

In this model one assumes that the spectrum can be explained by two inequivalent Te sites. Since the linewidth of the components is comparable to the splitting between them, the two pairs of quadrupole doublets are not well resolved. The significant parameter is the average QS,

$$\langle\Delta\rangle = \sum_i N_i\Delta_i / \sum_i N_i \quad , \tag{1}$$

where N_i and Δ_i designate the population and QS of the ith inequivalent site and any change in the isomer shift or in f factor between the two sites is assumed small.

If we assume the amorphous structure at $x = 0$ consists of predominantly two-fold coordinated Te, we can describe this structure as Te_n chains where n is unknown. Similarly, the structure at $x = 0.33$ is $GeTe_2$ (perhaps the tetrahedra shown in Fig. 10, but this identification is in no way required). Then, in our two-site model, we invoke structural separation of the system into molecular $GeTe_2$ based and Te_n based units. We leave open the question of the size of these units, but presumably they fall short of dimensions usually associated with a

macroscopic phase separation. Thus for the composition range $0 < x < 0.33$

$$Ge_xTe_{1-x} = xGeTe_2 + \frac{1-3x}{n} Te_n \quad (2)$$

Since each molecular unit of $GeTe_2$ has two equivalent Te sites, whereas Te_n has n equivalent Te sites, one may write

$$N_{i=1} = 2x$$

$$N_{i=2} = 1-3x$$

and this leads to

$$\langle\Delta\rangle = \frac{2x}{1-x} \Delta_{GeTe_2} + \frac{1-3x}{1-x} \Delta_{Te_n} \quad (3)$$

where Δ_{GeTe_2} and Δ_{Te_n} designate the QS's at $x = 0.33$ and 0. Fit A in Fig. 11 is a plot of Eq. (3) keeping $\Delta_{GeTe_2} = 7.8$ mm/sec and $\Delta_{Te_n} = 9.6$ mm/sec. In fit B Δ_{GeTe_2} is changed to 8.04 mm/sec for the annealed films. These fits are rather encouraging.

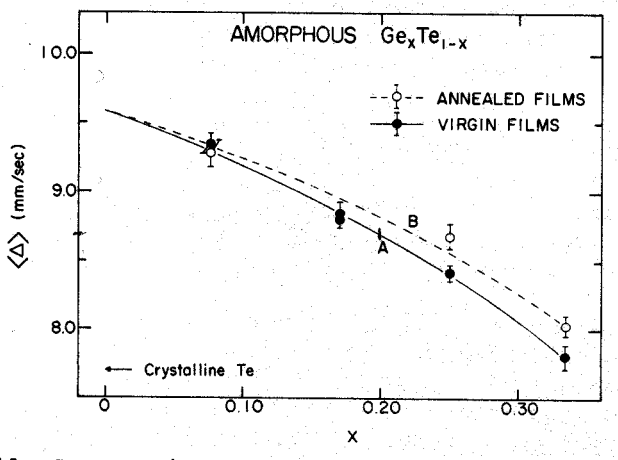

Fig. 11. Systematics of the mean quadrupole splitting $\langle\Delta\rangle$ for virgin and annealed films of Ge_xTe_{1-x} as a function of x for $0 < x < 0.33$. Curves A and B represent the two-site model constrained to agree with the data at $x = 0.075$ and $x = 0.33$.

In the composition range $0.33 < x < 0.50$, we again assume structural separation of the system into GeTe and $GeTe_2$ units, with all Te sites at $x = 0.33$ in a $GeTe_2$ surrounding and at $x = 0.5$ in a GeTe surrounding. Following the same development used above, we obtain:

$$\langle\Delta\rangle = \frac{(3x-1)}{1-x}\,\Delta_{GeTe} + \frac{2(1-2x)}{1-x}\,\Delta_{GeTe_2} \qquad (4)$$

This equation is plotted in Fig. 12. Curves A and B correspond to virgin and annealed films, respectively, with the values of Δ_{GeTe} and Δ_{GeTe_2} determined from measurements on virgin and annealed films of these compositions. The curves A and B do not describe the data well and curves C and D have been added to guide the eye. The nature of the discrepancy suggests that the failure of the two-site model in this region may be related to differences in the stabilities of the structures GeTe and $GeTe_2$ so that it is not permissible to treat them on an equal footing.

Effects of Annealing Amorphous Samples

Transport and optical properties of amorphous Ge_xTe_{1-x} films are known to exhibit large annealing effects. For example, Rockstad and deNeufville [21] have observed an almost 15% increase in the conductivity activation energy of virgin $GeTe_2$ films on annealing. This and other changes [23] observed in the bulk properties of these films have been attributed to thermally induced structural changes. The Mössbauer effect, on the other hand, provides a simple and direct technique for observing structural changes on a microscopic scale.

For the purpose of annealing and crystallizing the amorphous films, a furnace was assembled which provided for supporting the films between two flat surfaces during heating. The virgin films were sandwiched between two Al blocks, one of which was heated by a 40 watt heating tape. This assembly about 1 in. in diameter and 2 in. long was supported in an evacuated bell jar. The temperature of the Al blocks was monitored with an Fe-constantan thermocouple and it could be regulated to ± 3°C by means of a variac.

Virgin $GeTe_2$ films were annealed at 175°C for one hour in vacuum. Mössbauer spectra of virgin and annealed films

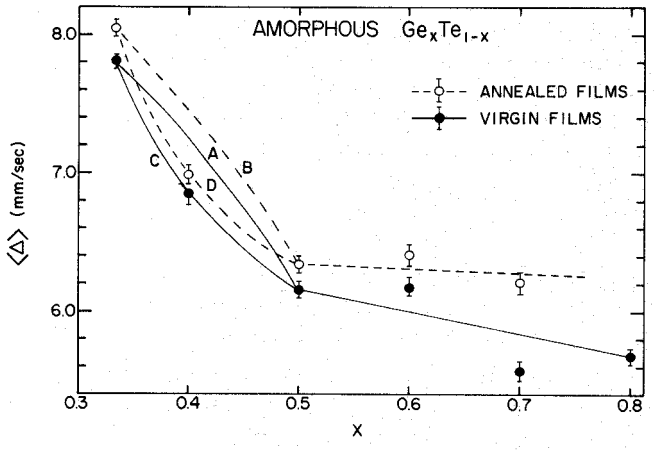

Fig. 12. Systematics of the mean quadrupole splitting for virgin and annealed films of Ge_xTe_{1-x} as a function of x for $0.33 < x < 0.50$. Curves A and B are the two-site model constrained to agree with the data at $x = 0.33$ and $x = 0.50$. Curves C and D are drawn to guide the eye.

were accumulated simultaneously in the experimental arrangement of Fig. 2. These measurements, summarized in Fig. 13, were performed for several film thicknesses on both virgin and annealed amorphous films. In both cases the linewidths extrapolated to zero absorber thickness are larger than the minimum observable linewidth $2\Gamma_n$. This suggests the presence of a distribution of QS's in both of these non-crystalline hosts. However, annealed $GeTe_2$ films exhibit an extrapolated linewidth which is approximately 0.4 mm/sec narrower than that observed for virgin $GeTe_2$ films. Thus, the process of annealing leads to a better defined QS. We also note that the magnitude of the QS increases by 0.2 mm/sec on annealing. The slope of the straight line obtained in a plot of Γ_{exp} vs. film thickness is a measure of the absorber f factor. The measurements in Fig. 13 indicate that the process of annealing leads to a two-fold increase in the f factor.

These large changes in the Mössbauer parameters on annealing $GeTe_2$ reflect a predominantly nearest neighbor effect. We suggest that the process of annealing leads to a greater degree of structural order in the local $GeTe_2$ structure.

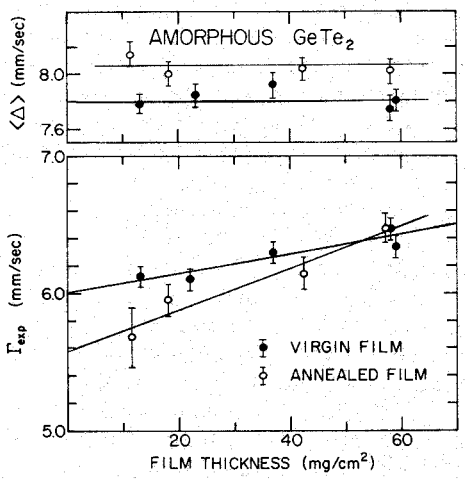

Fig. 13. Systematics of the mean quadrupole splitting $\langle\Delta\rangle$ and the experimental linewidth Γ_{exp} as a function of film thickness for virgin and annealed films of amorphous $GeTe_2$. Note the two-fold increase in the f value of amorphous $GeTe_2$ on annealing. (The f value is proportional to the slope of the Γ_{exp} versus thickness curve.)

The excess linewidth of about 0.4 mm/sec above $2\Gamma_n$ observed for the quadrupole components of annealed $GeTe_2$ films raises some interesting questions. The possibility exists that the heat treatment used did not complete the process of structural ordering. An alternative explanation would attribute the broadening to the influence of more distant neighbors.

Measurements on annealed Ge_xTe_{1-x} films were also performed at compositions other than $GeTe_2$. The $\langle\Delta\rangle$'s obtained from these measurements are shown in Figs. 11 and 12 along with similar data on virgin films. Over a broad range of compositions annealed films exhibit a somewhat larger $\langle\Delta\rangle$.

We note the absence of annealing effects in the most Te rich alloy studied ($x = 0.075$). This feature is not peculiar to Mössbauer measurements alone [21] and further suggests the presence of a low coordination Te site.

The independence of $\langle\Delta\rangle$ on x for $x > 0.5$ shows up better in the annealed films. While one can certainly extract a value of $\langle\Delta\rangle$ from the data in the range $0.5 < x < 0.7$, the values are less reliable because of the broad linewidths and small splittings. Nevertheless, we believe than an unstable amorphous structure tends to occur in this composition range. This structure is apparently very sensitive to sample preparation, and annealing the virgin films always leads to a definite value of $\langle\Delta\rangle$. Thus, we feel that the scatter in the data from virgin films reflects partial structural separation of Ge_xTe_{1-x} into amorphous GeTe and Ge, whereas the unique value of $\langle\Delta\rangle$ found in the annealed films results from complete structural separation into these components as given by

$$Ge_xTe_{1-x} = (1-x)\,GeTe + (2x-1)\,Ge$$

Such a model would explain the independence of $\langle\Delta\rangle$ and the isomer shift $\langle\delta\rangle$ on x.

Amorphous to Crystalline Phase Transformation

Amorphous Ge_xTe_{1-x} films are characterized by a well defined glass transition temperature T_g, above which they crystallize and exhibit long range order. This transition is exothermic [24] and one can generally establish it by measuring specific heats or by differential thermal analysis [23]. The variation of T_g as a function of composition for Ge_xTe_{1-x} has been studied by deNeufville [24] and these systematics exhibit an anomaly at $x = 0.33$.

Spectra of crystalline Ge_xTe_{1-x} alloys for some compositions are reproduced in Figs. 5, 6 and 7. The crystalline films were obtained by heating the amorphous films to a temperature 15°C above T_g in vacuum. At the composition $x = 0.075$, the spectrum is characterized by a QS which agrees well with that in Te metal. As the Ge content increases, the spectral intensity at zero velocity builds up until one reaches $x = 0.5$, where the spectrum acquires a simple Lorentzian lineshape. The fits shown for spectra at the compositions $x = 0.075$, $x = 0.17$, and 0.33 comprise these lines: a quadrupole doublet having a QS and isomer shift equal to that in Te metal and a single line at zero velocity. The interpretation of these spectra thus places Te in two inequivalent sites, one as in Te metal and the

other as in GeTe. Thus, the asymmetry of the spectrum at $x = 0.17$ results from a positive isomer shift of the Te metal doublet relative to the GeTe singlet. To summarize, for $x < 0.5$ the amorphous to crystalline phase transition in the Ge_xTe_{1-x} system leads to phase separation into crystalline GeTe and Te metal:

$$a\text{-}Ge_xTe_{1-x} \rightarrow (1-2x)\,c\text{-}Te + x\ c\text{-}GeTe$$

where a and c stand for amorphous and crystalline.

Amorphous Te

The most Te rich amorphous Ge_xTe_{1-x} alloy investigated corresponded to $x = 0.075$. There is a practical difficulty [15,19,20] in retaining the amorphous phase for compositions $x < 0.075$ at room temperature, although it may be possible to avoid crystallization with special techniques. Mössbauer parameters for the extremum composition $x = 0$ are of particular interest as these correspond to the amorphous phase of Te. One infers from the present data that in amorphous Te, there exists a substantially larger (24%) quadrupole splitting and a smaller isomer shift than for the crystalline form. As discussed previously, the data indicate that in the amorphous structure Te is located in chemical surroundings that are quite different from those of crystalline Te. Similar results are obtained from NMR measurements [15] on rapidly solidified Te and more recently from electron rdf results on evaporated Te [19]. These authors have described amorphous Te to consist of broken helical chains which average about six to seven atoms long. We have shown that this picture in itself is incomplete, and that a necessary ingredient of the structure is that the bond length in the amorphous chains is shorter than in crystalline Te.

Lucovsky and White [25] have recently advanced some considerations based on chemical bonding and bond lengths in amorphous semiconductors. They have stressed that the chemical binding of second neighbors becomes progressively stronger in going from crystalline S to Se to Te. In trigonal Te, second neighbors are located in adjacent helical chains. In amorphous Te the correlation between chains is presumably destroyed. We feel this must affect the geometry of the chains.

DISCUSSION AND SUMMARY

The structural picture [5] of amorphous Ge_xTe_{1-x} alloys that has emerged over the years from X-ray RDF, NMR and transport measurements, briefly is the following. Addition of Ge to amorphous Te leads to crosslinking of the Te chains and this process goes on until the composition $x = 0.33$ is reached where only Ge-Te bonds exist in the $GeTe_2$ structure. As this crosslinking process continues three types of Te environments emerge: One which has two Te near neighbors as in amorphous Te, a second which has one Te and one Ge near neighbor, and a third which has two Ge near neighbors as in $GeTe_2$. Formally, in our description of the average quadrupole splitting $\langle\Delta\rangle$ as a function of composition in the range $0 < x < 0.33$, we have considered only two inequivalent sites. The simplicity of the model and the resulting fit to the data in this range might seem to justify our approach. However, more complicated approaches should also lead to reasonable agreement with the data for $0 < x < 0.33$.

In the composition range $0.33 < x < 0.5$, the inadequacy of the two-site model indicates that the GeTe and $GeTe_2$ structural units probably cannot be treated on an equal footing.

The isomer shifts of amorphous and crystalline GeTe were found to be nearly the same within the limits of experimental error. Indeed, recent XPS measurements of Shevchik et al. [8] show that the valence band structures of amorphous and crystalline GeTe are almost identical. We feel that these observations can be generally reconciled with the 3-fold coordination of GeTe in the black phosphorus structure, a model recently advanced by Bienenstock [22] to reinterpret the X-ray RDF measurements. A particularly attractive feature of this model is that Te is bonded to three first and three second neighbor Ge atoms in a coordination that is quite distorted from cubic symmetry. The process of crystallization of amorphous GeTe can be visualized as one that leads to a rearrangement of the first and second neighbors to form an almost octahedral coordination around Te. The preservation of coordination number in the two Te phases may be responsible for the unchanged isomer shift and valence band structure while the symmetry rearrangement leads to dramatic changes in the electric field gradient as observed.

Finally, the sizable linebroadening of the quadrupole components (Tables II, III) in amorphous GeTe persisted in annealed samples as well. Virgin GeTe films were annealed at 150°C for a 24-hour period. For this particular composition we are inclined to believe that the heat treatment used did not saturate the process of structural ordering. From a thermodynamic viewpoint, it would appear impossible to completely anneal samples at this composition since the annealing temperature T_g is estimated [18] to be about 50°C higher than T_x. We therefore associate the broad linewidths to a distribution of quadrupole splittings resulting from a certain degree of structural disorder.

ACKNOWLEDGEMENTS

We wish to thank Ron Nowicki for help in preparing the samples and Ned Dixon, Yusuf Mahmud, Art Wagner and Jim Oberschmidt for assistance in the experimental and computational work. In the earlier phase of these experiments, performed at the University of Cincinnati, the interest of Professor K. L. Chopra in making available some samples of GeTe is gratefully acknowledged. We are especially grateful to Professor Arthur Bienenstock of Stanford University for valuable discussions on the Ge_xTe_{1-x} system and to C. W. Seidel of New England Nuclear Corporation for assistance in some aspects of the source preparation. One of us (P.B.) would like to thank the nuclear group at Stanford University for the warm hospitality extended him during his stay.

REFERENCES

1. P. Boolchand, Nucl. Instr. and Meth. 114: 159 (1974).
2. J. Oberschmidt and P. Boolchand, Phys. Rev., in press.
3. C. Hohenemser and R. Rosner, Nucl. Phys. A109: 364 (1968).
4. E. Gerdau, W. Räth and H. Winkler, Z. Physik 257: 29 (1972).
5. N. F. Mott and E. A. Davis, Electronic Processes in Non-Crystalline Materials (Clarendon Press, Oxford, 1971).
6. F. Betts, A. Bienenstock, and S. R. Ovshinsky, J. Non-Cryst. Solids 4: 554 (1970), and references therein.
7. F. Betts, A. Bienenstock, D. T. Keating, and J. P. deNeufville, J. Non-Cryst. Solids 7: 417 (1972).

8. N. J. Shevchik, J. Tejeda, D. W. Langer, and M. Cardona, Phys. Rev. Letters 30: 659 (1973).
9. R. J. Blattner, L. K. Walford, and T. O. Baldwin, J. Appl. Phys. 43: 935 (1972).
10. A. Taylor and B. J. Kagle, Crystallographic Data on Metal and Alloy Structures (Dover, 1963).
11. C. N. King, W. A. Phillips, and J. P. deNeufville, Phys. Rev. Letters 32: 538 (1972).
12. D. Raj and S. P. Puri, Phys. Letters 29A: 510 (1969).
13. A. Wagner, MS Thesis, University of Cincinnati, 1974 (unpublished).
14. P. Boolchand, S. Jha, and B. L. Robinson, Phys. Rev. B2: 3463 (1970).
15. A. Koma, O. Mizuno, and S. Tanaka, Phys. Stat. Solidi B46: 225 (1971).
16. P. Boolchand, T. Henneberger, and J. Oberschmidt, Phys. Rev. Letters 30: 1292 (1973).
17. A. Bienenstock, F. Betts, and S. R. Ovshinsky, J. Non-Cryst. Solids 2: 347 (1970).
18. A. F. Wells, Structural Inorganic Chemistry (Clarendon Press, Oxford, 1962).
19. T. Ichikawa, J. Phys. Soc. Japan 33: 1729 (1972).
20. K. Bahadur and K. L. Chaudhary, Appl. Phys. Letters 15: 277 (1969).
21. H. K. Rockstad and J. P. de Neufville, 11th International Conference on Physics of Semiconductors (Polish Scientific Publishers, Warsaw, 1972) p. 68.
22. A. Bienenstock, J. Non-Cryst. Solids 11: 447 (1973).
23. R. K. Quinn and R. T. Johnson, Jr., J. Non-Cryst. Solids 12: 213 (1973).
24. J. P. deNeufville, J. Non-Cryst. Solids 8-10: 85 (1972).
25. G. Lucovsky and R. M. White, Phys. Rev. B8: 660 (1973).